Semi-interpenetrated network based on functional CO_2-sourced polycarbonate as solid electrolyte for long cycle life lithium battery

Farid Ouhib,[a§] Leire Meabe,[b§] Abdelfattah Mahmoud,[c] Bruno Grignard,[a] Jean-Michel Thomassin,[a] Abdelhafid Aqil,[a] Frederic Boschini,[c] Christine Jérôme,[a] David Mecerreyes,[b*] Christophe Detrembleur [a*]

Novel functional polycarbonates alternating oxo-carbonate moieties and polyethylene oxide segments are synthesized by the facile room temperature (rt) organocatalyzed polyaddition of CO_2-sourced bis(α-alkylidene carbonate)s (bis-αCCs) with polyethylene oxide diols. The effect of the polyethylene oxide molar mass on the ionic conductivity and on the thermal properties of the poly(oxo-carbonate)s are investigated. The best candidate shows a low glass temperature of -44°C and a high ionic conductivity of 3.75 * 10^{-5} S cm^{-1} at rt when loaded with 30 wt% bis(trifluoromethanesulfonyl)imide salt (LiTFSI) without any solvent. All solid semi-interpenetrated network polymer electrolyte (SIN-SPE) is then fabricated by UV-cross-linking of a mixture containing a specifically designed poly(oxo-carbonate) bearing methacrylate pendants, diethylene glycol diacrylate and the previously described optimal poly(oxo-carbonate) containing LiTFSI. The resulting self-standing membrane exhibits a high oxidation stability up to 5 V (*vs* Li/Li^+), an ionic conductivity of 1.1 * 10^{-5} S cm^{-1} at rt and 10^{-4} S cm^{-1} at 60°C, and promising mechanical properties. Assembled in a half cell configuration with $LiFePO_4$ (LFP) as cathode and lithium as anode, the all-solid cell delivers a discharge capacity of 161 mAh g^{-1} at 0.1C and 60°C, which is very close to the theoretical capacity of LFP (170 mAh g^{-1}). Also, a stable reversible cycling capacity over 400 cycles with high coulombic efficiency of 99 % is noted at 1C. Similar results are obtained at rt provided that 10 wt% of tetraglyme was added to SIN-SPE.

I. Introduction

Today, the development of safe and efficient electrochemical devices for the storage of energy generated by intermittent renewable sources has become a strategic driver for ecologic transition.[1,2] As the result of their high specific energy and energy density, Li-ion batteries (LIBs) have emerged as key players for tackling this major challenge.[3] However, these devices are generally using mixtures of (a)cyclic organic carbonates in combination to lithium salts as liquid electrolytes. These liquids are causing some important safety issues such as flammability and the release of toxic products when the battery is damaged.[4] To surpass these hurdles, solid polymer electrolytes (SPEs) doped with a lithium salt are promising alternatives to organic liquid electrolytes[5,6,7] and are expected to become key structural elements for the next generation of high performance and safe all-solid batteries.[8] Ideal SPEs should display specific features such as (1) a good ionic conductivity (> 10^{-4} S. cm^{-1} at room temperature (rt)) to ensure ions transport and rapid charge/discharge, (2) a Li^+ transference number close to unity in order to reduce the concentration polarization of salts during operation and to produce high power density,[9] (3) suitable mechanical properties for elastic and flexible all-solid batteries that will prevent the formation of metal dendrites responsible for short circuits, and (4) a wide electrochemical stability window (up to 4-5 V *vs* Li/Li^+) to be compatible with both electrode materials and to prevent its degradation during battery operation.

Poly(ethylene oxide) (PEO) mixed with lithium salt is the most popular SPE used in battery applications.[10,11] The polar ether oxygen atoms of PEO dissociates the salt and Li^+ cations are transported by the segmental motion chains, mainly in the amorphous phase.[12,13] However, the major drawbacks of PEO-based SPEs are their low Li^+ transference number (< 0.2), modest ionic conductivity at room temperature (< 10^{-5} S cm^{-1}) and narrow electrochemical stability (< 4 V *vs* Li^+/Li).[14] Moreover, their poor mechanical properties resulting from the plasticization of PEO by the dissolved organic salt and its low melting temperature are not sufficient to avoid short circuits between the two electrodes. In the quest for high performance SPEs, some research groups have demonstrated the benefit of introducing carbonate moieties within the main PEO chains on the ionic mobility.[15] The large dipole moment of the carbonates improved the salt dissociation and increased the segmental motion ability of the copolymers chains, yielding ionic conductivity values higher than 10^{-5} S cm^{-1} at rt. However, these solid electrolytes, synthesized by copolymerization of dimethyl carbonate with poly(ethylene oxide) diol at high temperature (180°C), are sticky materials that cannot by handled as self-standing membranes for lithium battery applications. The partial decarboxylative ring-opening polymerization of 5-membered cyclic carbonates and the ring-opening copolymerization of CO_2 with epoxides are elegant and facile approaches to design poly(ether-*co*-carbonate)s for potential SPE applications.[16,17] However, the difficulty to introduce functional groups within/along the poly(ether-*co*-carbonate)s backbone is a key issue for tailoring self-standing membranes SPE of appropriate mechanical resistance. Recently, some of us introduced a novel and versatile route to functional polycarbonates, poly(β-oxo-carbonate)s, by facile room

temperature organocatalyzed polyaddition of CO_2-sourced bis(α-alkylidene carbonate)s (bis-αCCs) with diols.[18] Herein, we exploit this toolbox to synthesize an unprecedented self-standing SPE membrane that is evaluated in Li/$LiFePO_4$ cell. We demonstrate that poly(ß-oxo-carbonate)s alternating flexible PEO sequences and oxo-carbonate groups present a high ionic conductivity at rt. By adapting the synthetic procedure, we also prepared in a simple one-pot process poly(ß-oxo-carbonate) bearing pendant cross-linkable methacrylates. The two polymers are then processed into a semi-interpenetrated polymer networks (SIN) with improved mechanical properties and high electrochemical stability. The performances of this SIN in Li/$LiFePO_4$ cell are evaluated at 60°C and at rt.

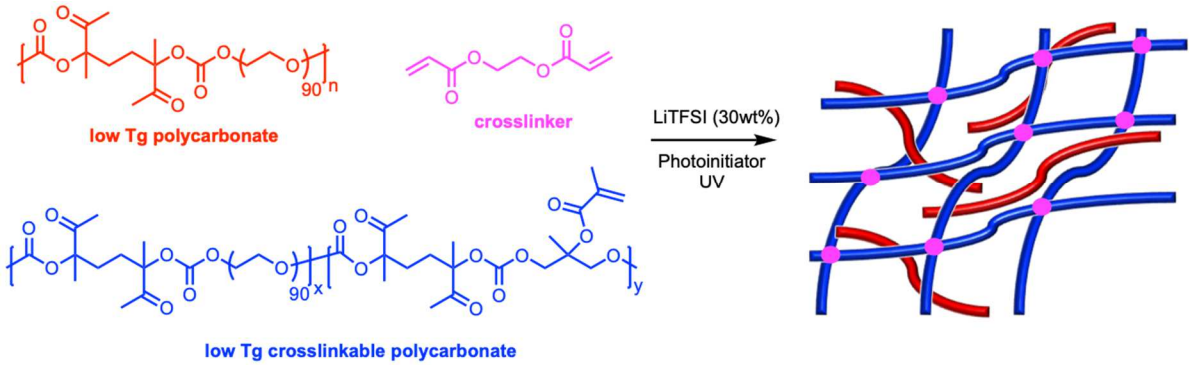

Scheme 1: General strategy for the design of solid semi-interpenetrated polymer electrolytes from novel CO_2-sourced poly(β-oxo-carbonate)s

II. Experimental Section

II.1 Materials and synthetic part

Poly(ethylene glycol) (M_n = 1500 g mol^{-1}), poly(ethylene glycol) (M_n = 2000 g mol^{-1}), poly(ethylene glycol) (M_n = 4000 g mol^{-1}) and diethyleneglycoldiacrylate (99%) were purchased from Aldrich. 1,8-Diazabicyclo[5.4.0]undec-7-ene (DBU, 99%) were purchased from Fluorochem. Lithium bis(trifluoromethane)sulfonimide (LiTFSI) (99.9%) was supplied from Solvionic and used as recieved. *Meso*-4,4-dimethyl-5-methylene-1,3-dioxolan-2-one (bis-αCC) was synthesized as reported elsewhere by our group.[18] 1,3-dihydroxy-2-methylpropan-2-yl methacrylate was synthesized as reported in the literature.[19]

General synthetic procedure for PEO/poly(β-oxo-carbonate) :
In a typical experiment for PC-1, 200 mg of bis-αCC (0.787 mmol, 1 eq) and 1181 mg (0.787 mmol, 1 eq) of poly(ethylene glycol) (M_n = 1500 g mol^{-1}) were added in reaction tube with 1.3 mL of dry DMSO. 0.2 ml (0.04 mmol, 0.05 eq) of DBU solution (C = 0.2 M in DMSO) was added and the reaction medium was stirred at 25°C. After 24h, the obtained polymer was purified by double precipitation in diethyl ether. The purified polymer was dried under vacuum a 60°C (1284 mg, 93 % of yield).
PC-2 and PC-3 were synthesized with same procedure. ^1H and ^{13}C-NMR spectra are reported in supporting information.
Synthesis of crosslinkable PC (PC-4): 200 mg of bis-αCC (0.787 mmol, 1 eq), 68 mg (0.393 mmol) of 1,3-dihydroxy-2-methylpropan-2-yl methacrylate and 1574 mg (0.393 mmol, 1 eq) of poly(ethylene glycol) (M_n = 4000 g mol^{-1}) were added in reaction tube with 1.8 ml of dry DMSO. 0.2 ml (0.04 mmol, 0.05 eq) of a DBU solution (C = 0.2 M in DMSO) was added and the reaction medium was stirred at 25°C. After 24h, the obtained polymer was purified by double precipitation in diethyl ether. The purified polymer was dried under vacuum at room temperature (1602 mg, 89 % of yield).

Preparation of polymer electrolytes
Solid poly(oxo-carbonate) Electrolyte. 70 mg of aliphatic poly(β-oxo-carbonate) and 30 mg of LiTFSI were dissolved in 1 mL of acetone. After 1 h of mixing, the solvent was evaporated at room temperature followed by a thermal treatment of 24 h at 60 °C.
All solid cross-linked SPE. 60 mg of PC-3, 20 mg of cross-linkable polycarbonate (PC-4), 20 mg of diethylene glycol diacrylate, 42.85 mg of LiTFSI and 3 mg of 2-hydroxy-2-methylpropiophenone (photoinitiator) were dissolved in 1 mL of acetone. After 1 h, the solution was casted onto a silicon mold. The solvent was removed at ambient conditions followed by a high vacuum treatment. Finally, the films were passed 3 times under a xenon arc lamp (Helios Italquartz, 45 mW cm^{-2}). Before performing electrochemical characterization, the SPEs were dried under vacuum at rt during 24 h, followed by increasing the temperature up to 60 °C for 2h.

II.3 Characterization methods

Nuclear magnetic resonance (NMR) spectroscopy. ^1H and ^{13}C NMR analyses were performed on Bruker Avance 250 or 400 MHz spectrometers in $CDCl_3$, DMSO or DMF at 25 °C in the Fourier transform mode. 16 or 64 scans for a ^1H spectra and 512 or 2048 scans for ^{13}C spectra were recorded.
Gel permeation chromatography (GPC). Number-average molecular weight (Mn) and dispersity (Đ) of the different polymers were determined by size exclusion chromatography (SEC) in THF at 45 °C at a flow rate of 1 mL/min with a Viscotek 305 TDA liquid chromatograph equipped with two PSS SDV linear M columns calibrated with poly(methyl methacrylate) standards and a refractive index detector.
Differential Scanning Calorimetry (DSC) was performed on a DSC Q2000 differential calorimeter (TA Instruments). All the experiments

were performed under ultrapure nitrogen flow. Samples of 5-8 mg were used. Measurements were performed by placing the samples in sealed aluminium pans. The samples were first heated at a rate of 20 K min^{-1}, from 30 °C to 100 °C and they were left 3 min at 100 °C to eliminate the thermal history. Subsequently, the samples were cooled down to -70 °C at a rate of 10 K min^{-1} and subsequently heated to 100 °C at 10 K min^{-1} after waiting at -70 °C during 3 min. Once again, the samples were cooled at a rate of 50 K min^{-1} until -70 °C, and later it was heated up at 20 K min^{-1} up to 100 °C, in order to determine the glass transition.

Rheological measurements were performed using an ARES-G2 Rheometer from TA Instruments equipped with an ARES-G2 curing accessory, made of a light guide, a quartz plate and a reflecting mirror assembly allowing the transfer of the UV irradiation from the UV-light source to the sample. UV curing at 365 nm was performed with an OmniCure Series 2000, 200 W, 365 nm. Typically, 60 mg of aliphatic polycarbonate, 20 mg of cross-linkable polycarbonate, 20 mg of diethylene glycol diacrylate, 42.85 mg of LiTFSI and 3 mg of 2-hydroxy-2-methylpropiophenone (ultraviolet initiator), were dissolved in 1 mL acetone. After stirring during 1 h, the solutions were casted onto the rheometer plates. The solvent was removed under ambient conditions and later, by applying a high vacuum (disc with 1 mm of diameter and 0.2 mm). The time evolutions of the elastic and viscous moduli were recorded at a frequency of 1 Hz and a strain of 1% without and under UV irradiation at 365 nm.

The *ionic conductivity* was studied by electrochemical AC impedance spectroscopy (EIS) with an Autolab 302N potentiostat galvanostat with temperature controlled by a Microcell HC station. The membranes were placed between two stainless steel electrodes and sealed in a Microcell under inert atmosphere in a globe box (M-Braun) to avoid the contact of the sample with moisture. The frequency range was set from 0.1 MHz to 0.1 Hz and the amplitude was 10 mV. In all the cases the average surface area of the electrode was 0.5026 cm^2. For the characterization of lithium transference number and electrochemical stability were closed in CR2032 and they were measured in an Autolab 302N potentiostat galvanostat. For the lithium transference number the SPE was sandwiched between two lithium disks, whereas for electrochemical stability between lithium disk and a stainless steel (SS) electrode. Before the analysis, the coincells were left to stabilize at 70 °C for 24 h. Lithium transference number was calculated based on Bruce and Vincent method at 70 °C [1]. Electrochemical stability window was determined by applying cyclic voltammetry (CV) of the polymer electrolyte at 70 °C. The anodic limit was evaluated between open circuit potential (OCV) and 5.5 V vs. Li^+/Li at a constant rate of 0.5 mV s^{-1}.

The electrochemical stability of the electrolyte membranes and *battery performances* were conducted in two-electrode coin cells, using $LiFePO_4$ (LFP) as working electrode, Li metal (Aldrich) as counter and reference electrode, and solid poly(β-oxo-carbonate) (**PC-1, PC-2, PC-3)** as solid electrolyte. The positive electrode was prepared by dispersing 60 wt % of $LiFePO_4$, 20 wt % conductive carbon (Super P), and 20 wt % of poly(β-oxo-carbonate) **PC-3** as binder in acetone under stirring for 2h. The resulting slurry was coated on aluminum foil with a thickness of 120 µm and then dried at 50 °C in vacuum for 8 h. Discs of 1.2 cm in diameter, containing 1–2 mg/cm^2 of $LiFePO_4$ were cut. For the preparation of all-solid cross-linked SPEs (**SIN-PC-3**), 600 mg of **PC-3**, 200 mg of cross-linkable polycarbonate **PC-4**, 200 mg of diethylene glycol diacrylate, 420 mg of LiTFSI and 30 mg of 2-hydroxy-2-methylpropiophenone (photoinitiator) were dissolved in 2 mL of acetone. After 1 h, the solution was casted onto a teflon mold. The acetone was removed under ambient conditions followed by a high vacuum treatment. Finally, the films were passed 3 times under a xenon arc lamp (Helios Italquartz, 45 mW cm^{-2}). Before battery assembly, the SPEs were dried under vacuum at rt during 24 h. Discs of 1.4 cm in diameter (~ 100 µm of thickness) were cut. Cross-linked SPEs **SIN-PC-3** with TEG were prepared according to the same procedure and by adding 120 mg of tetraglyme to the mixture of 600 mg of **PC-3**, 200 mg of cross-linkable polycarbonate **PC-4**, 200 mg of diethylene glycol diacrylate, 420 mg of LiTFSI and 30 mg of 2-hydroxy-2-methylpropiophenone. **SIN-PC-3** based electrolyte was sandwiched between metallic lithium and the working electrode. CR2032 coin cells were assembled under argon in the glove box. The galvanostatic charge/discharge curves were measured using a multichannel Biologic potentiostat (VMP3) between 2.5 and 4.2 V *vs.* Li^+/Li^0 at different cycling rates C/n (1 Li per f.u. in n hours). Cycling galvanostatic measurements were conducted under thermostatic conditions at 25±0.5 and at 60 ±1 ◦C. For the rate capability, the cells were cycled at charge/discharge rates from 0.1 to 1 C. After the rate capability study, the cells were subjected to cycle back at the lower rate (0.5C) for 4 cycles to test if the reduction of capacity at the highest rates is reversible, which gives an indication of the stability of the electrolyte polymer at high current densities. All over the manuscript, the capacity is refereed to mass of $LiFePO_4$ in the composite cathode.

III. Results and Discussion

Synthesis and characterizations of poly(oxo-carbonate)s. As illustrated in Scheme 2, three poly(oxo-carbonate)s were synthesized by DBU organocatalysed polyaddition of bis-αCC with PEO diol of various molar masses (1500, 2000 and 4000 g/mol) at rt in DMSO. The structure of the regioregular poly(oxo-carbonate)s, noted **PC-1** (prepared from PEO 1500 g/mol), **PC-2** (prepared from PEO 2000 g/mol) and **PC-3** (prepared from PEO 4000 g/mol), were confirmed by ^{1}H- and ^{13}C-NMR spectroscopy (Figures S1 and S2). ^{1}H-NMR spectra of the three polymers show the characteristic peaks of the methylene proton adjacent to the carbonate groups at 4.2 ppm and the peak of the methyl in α position of the ketone groups at 2.15 ppm. The apparent molar masses (M_n) of the purified copolymers were determined by size exclusion chromatography (SEC) in THF as eluent and by using PEO standards. All polymers showed high M_n values of 45,000 to 60,000 g/mol and dispersities of 1.5-1.6. All macromolecular characteristics of the polymers, as well as their thermal properties, are summarized in Table 1.

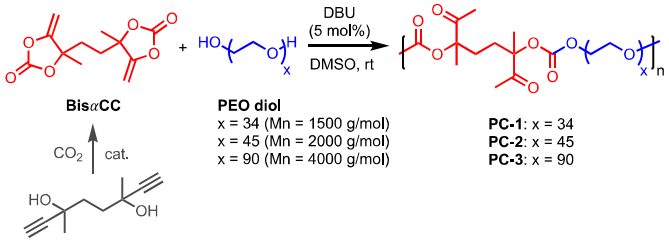

Scheme 2: Reaction scheme for poly(oxo-carbonate)s.

Table 1: Molecular characteristics and thermal properties of poly(oxo-carbonate)s.

Entry	M_n of PEO (g/mol)	M_n (g/mol)	D	T_g (°C)	T_m (°C)	ΔH_f (J/g)
PC-1	1,500	60,000	1.66	-43	23	56
PC-2	2,000	45,000	1.55	-52	31	60
PC-3	4,000	49,000	1.53	-52	41	67

The thermal properties of the three copolymers (Figure S3), evaluated by DSC, showed a semi-crystalline behavior with a melting temperature (T_m) of 23°C for **PC-1** that increased up to 41°C for **PC-3** (Table 1). All copolymers exhibited a low glass transition temperature (T_g) that decreased from -43°C for **PC-1** to -52°C for **PC-2** and **PC-3**. These thermal properties are mainly dictated by the PEO molar mass introduced within the copolymer chain.

Evaluation of poly(oxo-carbonate)s as solid polymer electrolytes (SPEs). We then prepared SPEs by mixing the different polymers (**PC-1-3**) with 30 wt% LiTFSI in acetone, followed by solvent removing. Based on our previous study, it was decided to include 30 wt% LiTFSI in the formulation. It seems that in PEO-PC systems, 30 wt% of salt is the optimum balance, giving the best electrochemical properties (Ref.). Their thermal properties and anhydrous ionic conductivities were evaluated by dynamic scanning calorimetry (DSC) and electrochemical impedance spectroscopy (EIS), respectively. The ionic conductivity of the three SPEs were evaluated at a temperature ranging from 100 °C to 25 °C. The results are depicted in Figure 2 and show a clear increase of the ionic conductivity with the PEO molar mass incorporated within the PC chain. These results indicates that a higher number of ethylene oxide units increase the segmental motion, which favor the ionic mobility. At 25°C, an ionic conductivity of 3.75 $\times 10^{-5}$ S.cm^{-1} was measured for **PC-3** which is 7.8 times higher than that obtained for **PC-1** (4.86 $\times 10^{-6}$ S. cm^{-1}). The ionic conductivity of **PC-3** (3.75 $\times 10^{-5}$ S.cm^{-1} at room temperature and 1.86 $\times 10^{-4}$ S.cm^{-1} at 60°C) is comparable or even better to those determined for the most efficient polycarbonate-based SPEs.[15,20,21,22,2324]

DSC curves of the three SPEs are shown in Figure 2b. All PCs were plasticized by LiTFSI, resulting in SPEs with suppressed or decreased melting temperature . The introduction of LiTFSI avoids the crystal formation and the materials results in amorphous SPEs. In PC-3 a small melting enthalpy can be observed at 30 °C. However, the ionic conductivity of PC-3 does not seem to be affected by the crystallinity. The glass transition has a bigger effect on the ionic conductivity. The T_g of SPEs decreased with the molar mass of PEO, from -37°C for **PC-1**, to -41°C for **PC-2** and to -44°C for **PC-3**. This result is in agreement with the highest ionic conductivity observed for **PC-3**. Despite its attractive ionic conductivity, **PC-3** based SPE was however a sticky material that could not form a self-standing membrane.

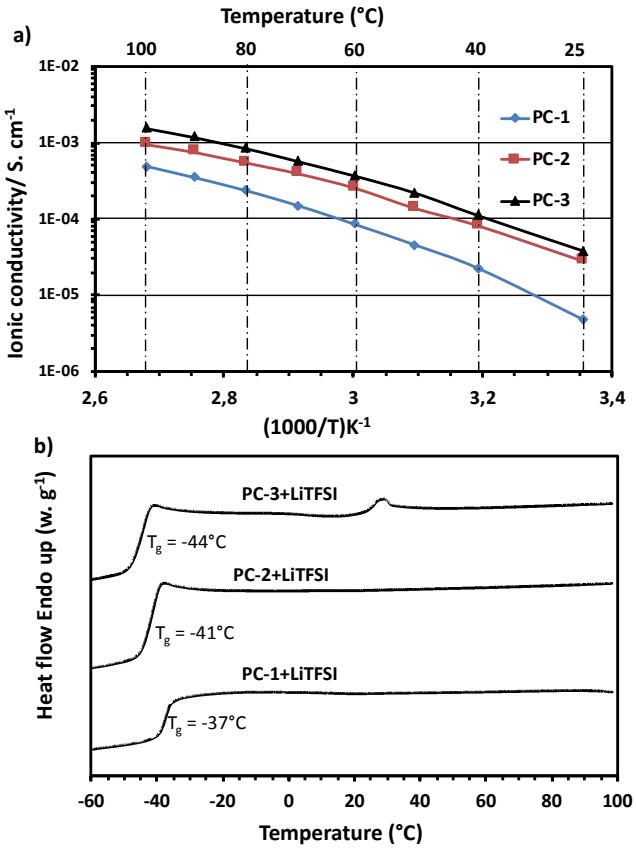

Figure 1: a) Arrhenius plot,temperature dependence of the ionic conductivity, b) DSC traces for the second heating of **PC-1**, **PC-2** and **PC-3** containing 30 wt% of LiTFSI.

Preparation and characterizations of self-standing SPEs membranes. In order to improve the SPE mechanical properties, we have prepared a semi-interpenetrated network (SIN) via photochemical crosslinking of a novel poly(oxo-carbonate) bearing methacrylate pendants (**PC-4**) with diethyleneglycol diacrylate, in the presence of **PC-3**, LiTFSI, and 2-hydroxy-2-methylpropiophenone as the photo-initiator (Scheme 1). The cross-linkable poly(oxo-carbonate) **PC-4** was designed to mimic **PC-3** that presented the highest ionic conductivity. It was prepared by the DBU organocatalysed polyaddition of bis-αCC with a mixture of diols, PEO diol (Mn = 4000 g/mol) and 1,3-dihydroxy-2-methylpropan-2-yl methacrylate (DHMPM), at rt in DMSO (Scheme 3). DHMPM was synthesized following the work of L.I Ronco. *et al.* (Ref.: L.I. Ronco, A. Basterretxea, D. Mantione, R.H. Aguirresarobe, R.J. Minari, L.M. Gugliotta, D. Mecerreyes, H. Sardon, Temperature responsive PEG-based polyurethanes "à la carte", Polymer, 122 (2017) 117-124). After 24h of reaction, **PC-4** was collected with 89% yield with a Mn

of 28000 g/mol and a dispersity of 1.5. Figure S3 shows the ^{1}H-NMR spectrum of the copolymer that confirms the copolymer structure and the incorporation of 48 mol% of methacrylate moieties within the polymer chains. The photopolymerization of diethylene glycol diacrylate and methacrylate pendant groups were verified by Fourier transform infrared spectra by the complete disappearance of the bands associated to the C=C double bonds of acrylates and methacrylates at 1600-1650 cm^{-1} after crosslinking (Figure S5).

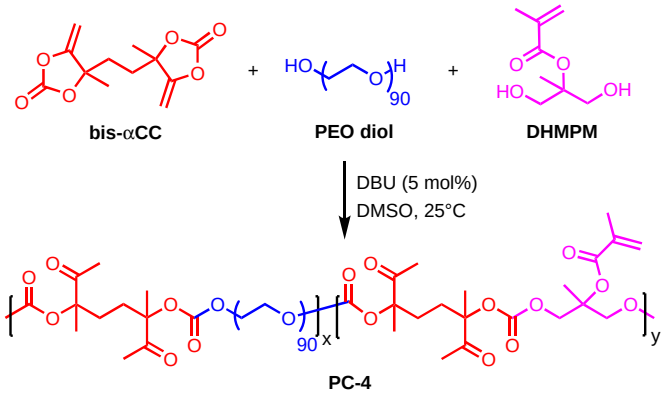

Scheme 3: Reaction scheme for crosslinkable poly(oxo-carbonate) **PC-4**.

The cross-linking reaction for the formation of SIN-SPE was then followed by rheology experiments (Figure 2a) on the following formulation: **PC-3** (41.4 wt%), LiTFSI (29 wt%), **PC-4** (13.8 wt%), diethylglycol diacrylate (13.8 wt%) and the photoinitiator (2 wt%). The elastic (G') and loss (G'') moduli of SIN-SPE, named **SIN-PC-3**, were measured as a function of time for 200 s in the dark, followed by 200 s under UV-irradiation at 365 nm at rt.

In the absence of UV-light, the loss modulus (G") is higher than the elastic modulus (G') as expected for a non-crosslinked polymer (Figure 2a). Upon UV light, both moduli drastically increased after few seconds of reaction, with G' that increased more rapidly (from 0.6 to 9.9 MPa) than G" (from 0.8 to 2.3 MPa). The cross-over point that was observed after about 20 s corresponds to the network formation, with G' values becoming much higher than G'' ones. A self-standing transparent membrane was collected after a few seconds of irradiation (Figure 2c).

This self-standing membrane presents enhanced mechanical properties compared to **PC-3**/LiTFSI SPE of the same LiTFSI content (30 wt%) with G' value as high as 8.5 MPa for **SIN-PC-3** vs 0.06 *10 $^{-8}$ MPa for **PC-3** at 0.01 rad.s^{-1}, Figure S6). **SIN-PC-3** presents appropriate mechanical properties and elasticity for the design of flexible solid electrolyte which can maintain a good interfacial contact and even could prevent the formation of lithium dendrites into lithium ions batteries devices.[25,26]

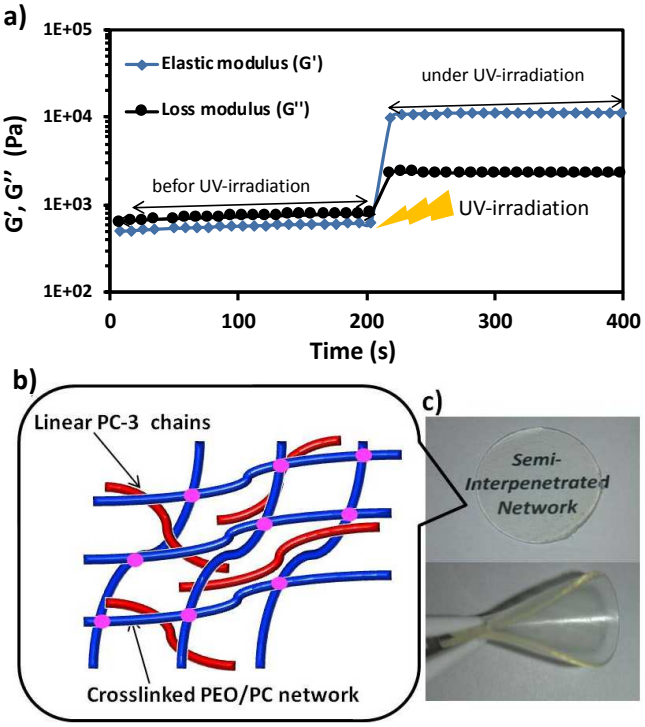

Figure 2: a) Elastic (G') and storage (G'') moduli, and complex viscosity of **SIN-PC-3** before and after UV-crosslinking, b) schematic representation and picture of the self-standing **SIN-PC-3** membrane.

The thermal properties and temperature dependence of ionic conductivity of **SIN-PC-3** was then measured in similar conditions than those previously used for **PC-3** based SPE (containing 30 wt% LiTFSI). As presented in Figure 3a, the ionic conductivity of **SIN-PC-3** (1.11×10^{-5} S. cm^{-1} at rt) was slightly lower than that measured for **PC-3** based SPE (3.75×10^{-5} S. cm^{-1} at rt), whereas Tg was only slightly affected (-42°C for **SIN-PC-3** *vs* -44°C for **PC-3** SPE; Figure 3b) by the formation of cross-linked network. This three-dimensional system will limit the chain mobility, and will cause a decrease on ionic conductivity respect to PC-3, which is not drastic decrease in our system. The formation of crosslinked network decreased the chain mobility of **PC-3** which can explain the ionic conductivity decreasing and T_g increasing……

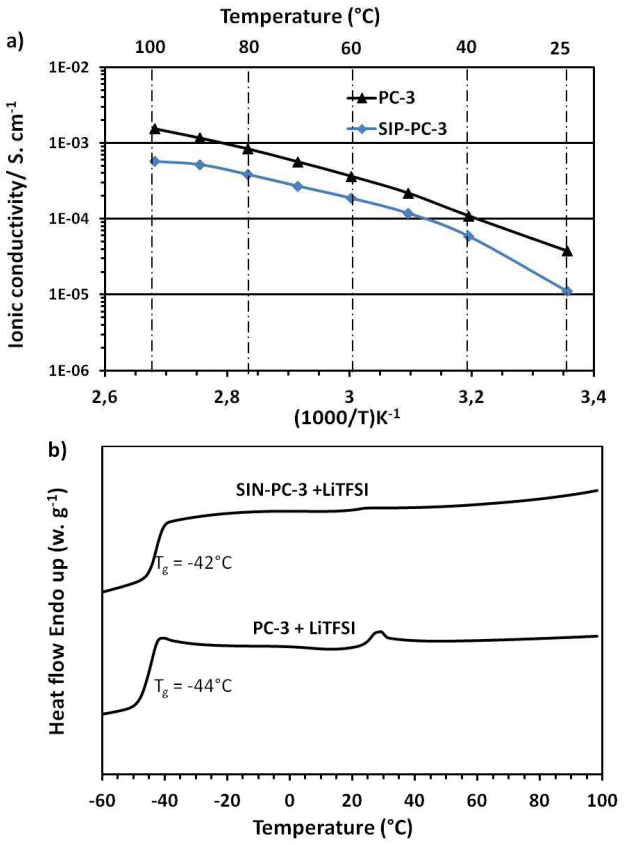

Figure 3: a) Arrhenius plot, Ttemperature dependence of ionic conductivity, b) DSC traces for the second heating of solid electrolyte based **SIN-PC-3** and **PC-3**.

The lithium transference number (t_{Li^+}) is used to describe Li^+ ion transfer ability in SPE, which is related to the rate capability of Li^+ in the electrolyte. It is accepted that carbonyl groups are able to dissociate the lithium cation from TFSI anion (REF:). Therefore, it will promote the lithium conduction. In order to demonstrate this,the cationic transference number (t_{Li^+}) calculated using Bruce and Vincent method at 70 °C was t_{Li^+}= 0.28 for **SIN-PC-3** (Figure S7), which is improved respect to reported value for PEO (t_{Li^+}= 0.20) (REF). This result is consistent considering the relation between ethylene oxide units and carbonate groups that we have in the polymer. Even though the effect of the carbonyl group is not as effective as it is in other polycarbonate based SPEs (REF:). Additionally, FTIR-ATR was used to confirm the coordination of lithium cation with carbonyl groups. A slight coordination of lithium with carbonyl groups can be detected from the analysis, which is the reason of improving the t_{Li^+} value, Figure S8.

The electrochemical stability window of **SIN-PC-3** was investigated by cyclic voltammetry (CV) at 70°C. As shown in Figure S8, **SIN-PC-3** was stable up to 5 V (*vs* Li^+/Li), demonstrating an enhanced electrochemical stability of our electrolyte compared to PEO-based SPE reported in the literature (REF). Consequently, **SIN-PC-3** appeared as a promising SPE candidate for Li battery with high positive active materials.

Electrochemical performances of all-solid state lithium battery. We then evaluated the polycarbonate-based semi-interpenetrated network SPE in an all-solid-state lithium battery. For that purpose, we fabricated a prototype half-cell by sandwiching **SIN-PC-3** between lithium metal as anode and lithium iron phosphate ($LiFePO_4$, LFP) as cathode, without any additional separator. Figures 4a and b present the charge-discharge profile and the rate performances of the Li/**SIN-PC-3**/LFP cell obtained at various rates, stepwise increased from 0.1 to 1C and returned to 0.5C at 60°C. The cell delivered a discharge capacity of 161 mAh g^{-1} at 0.1C which is very close to the theoretical capacity of LFP (170 mAh g^{-1}). The charge/discharge capacity did not drop much by increasing the C-rate. It was even possible to cycle at a C-rate of 1C with a discharge capacity of 102 mAh g^{-1}. When the current returned to 0.5C, the discharge capacity was back to 127 mAh g^{-1}, indicating good reversibility of the battery.

Figure 4a illustrates the long cycling performance of the cell at a current density of 1C at 60 °C. The cell delivered a first charge capacity of 99 mAh g^{-1}, and the discharge capacity was 97 mAh g^{-1}. This irreversible capacity during the first cycle might be related to the formation of a surface film at the cathode polymer electrolyte interface and other side reactions. From the second cycle, the coulombic efficiency maintained a constant value of 100%. After 400 cycles, the reversible capacity was still as high as 83 mAh g^{-1}, corresponding to about 86% of its initial capacity. This result confirms the long cycle life of the cell, and thus the good electrochemical stability of the poly(oxo-carbonate)-based solid electrolyte even at high temperature (60°C). Compared to other crosslinked polycarbonate or polyether based SPEs, **SIN-PC-3** exhibits competitive battery performances and stability at 60°C (REF).[272829 3031]

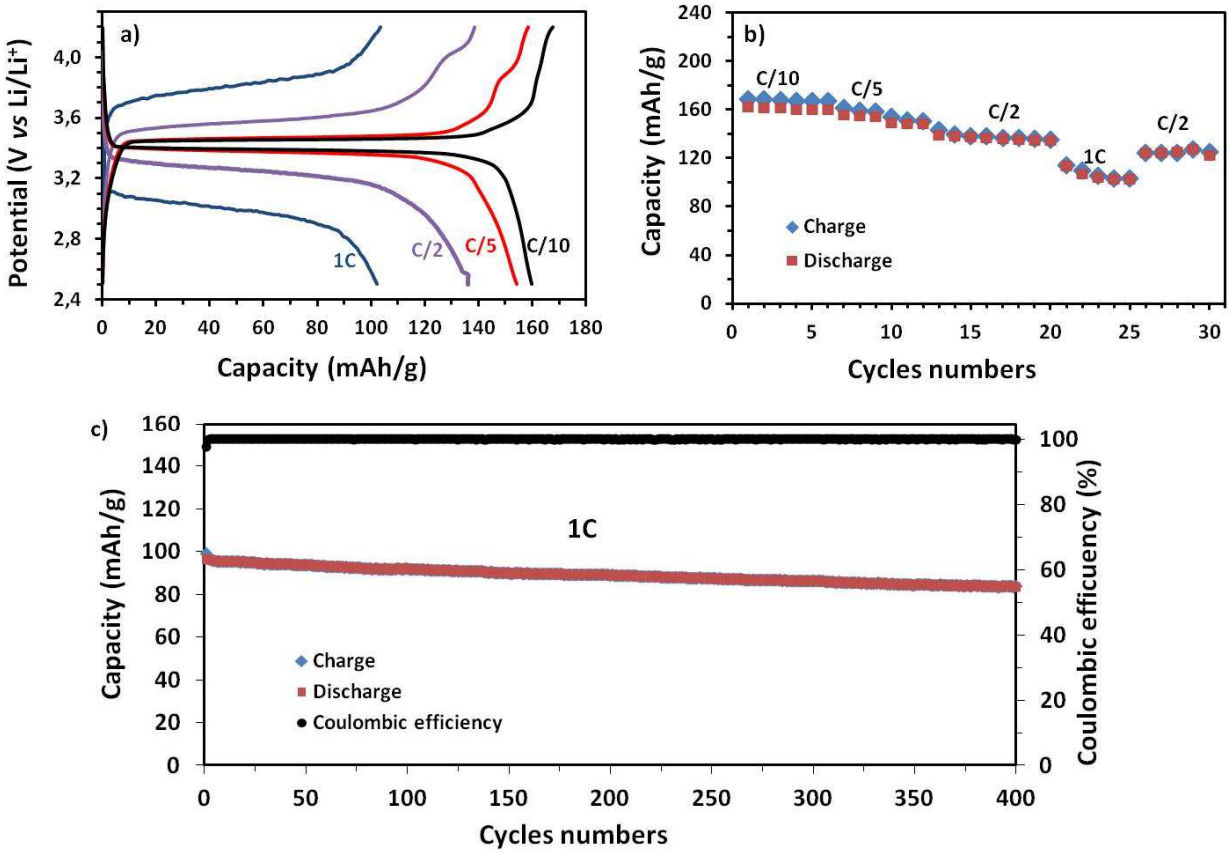

Fig. 4: Electrochemical performances of all-solid **SIN-PC-3**/Li/$LiFePO_4$ cell in the voltage range of 2.5-4.2V at 60°C. (a) charge–discharge profiles, (b) the reversible capacity at various current rates (C/10 to 1C) and (c) cycle performance of the cell at a current rate of 1C.

The same cell was however not cycling at rt. Indeed, the ionic conductivity of **SIN-PC-3** is not high enough for practical battery application at this temperature. One of the most popular approaches to improve the ionic conductivity of SPE consists in adding molecular plasticizers such as succinonitrile or low molecular weight PEG with methoxy end-groups.[32,33] Most of the works reports that large amounts of plasticizers (20 – 70 wt%) were required to significantly increase the ionic conductivity. However, these plasticizers negatively affected the mechanical properties and liquid leakage was also a risk during operation.[34] By adding a small quantity of tetraglyme (TEG) as a high boiling point and non-flammable additive (10 wt% *vs* all solid polymer) to **SIN-PC-3**, we enhanced the ionic conductivity at rt of our self-standing membrane (4.7×10^{-5} S. cm^{-1} *vs* 1.11×10^{-5} S. cm^{-1} at rt, Figure S9) without sacrificing their mechanical properties (Figure S10).

Assembled in half-cell configuration, excellent cycling performances were achieved for the cell with a discharge capacity of 86 mAh/g at 1C after 400 cycles at rt (Figure 5a). The cell exhibited excellent rate capabilities from C/10 to 1C, with a reversible capacity of 165 mAh g^{-1} at C/10 (corresponding to 97% of theoretical capacity of LFP) and 82 mAh g^{-1} at 1C (48% of theoretical capacity of LFP) (Figure 5b,c). These excellent rate performances are the result of TEG that plasticizes **SIN-PC-3**, consequently increasing the polymer chains mobility and facilitating the lithium ions diffusion.[35,36] This cell containing only 10 wt% of TEG presents comparable battery performances to similar cells prepared from SPE containing higher amounts of plasticizers (20 ~ 70%).[3738] [394041] Additionally, if we compared to another batteries containing carbonate groups in the SPE, clearly can be observed the improvement and advantages on capacity and C-rates provided by polymer electrolyte that we developed in this work (REF).

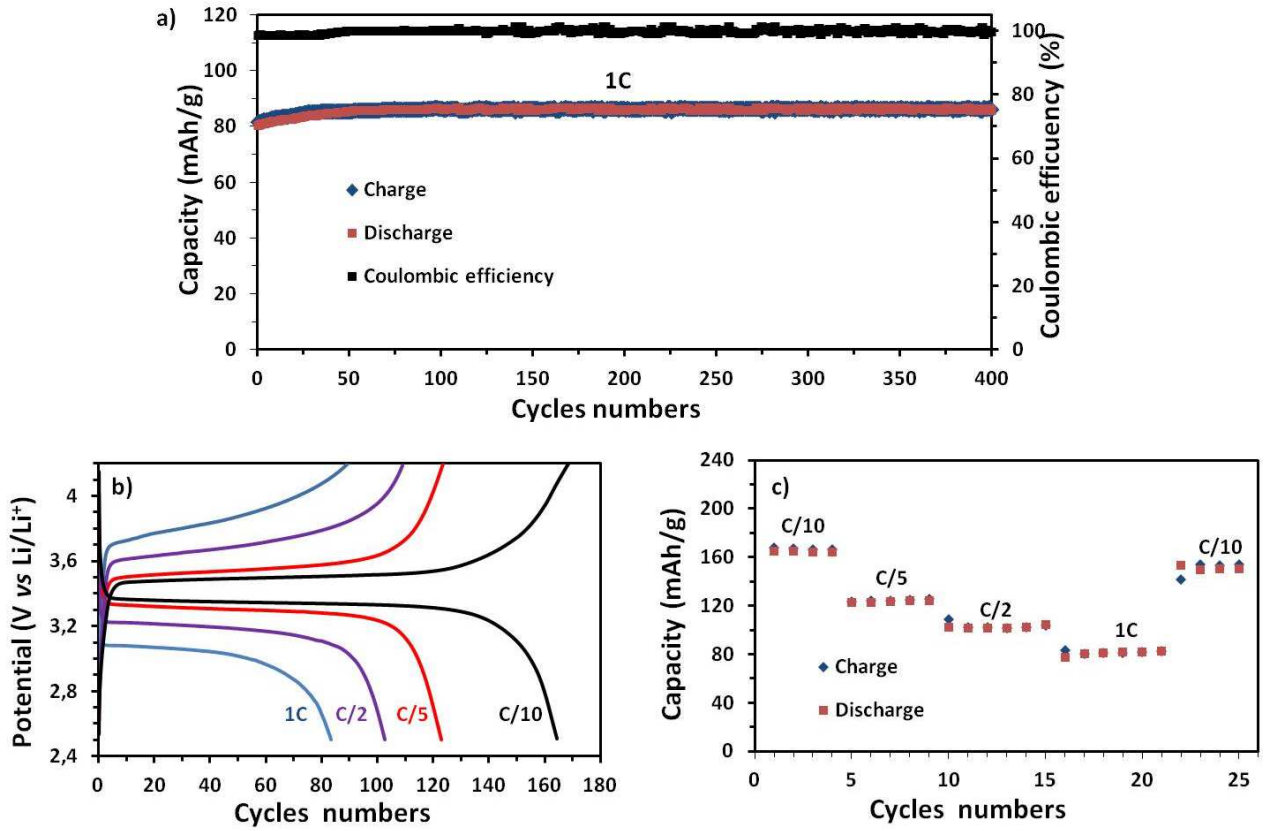

Fig. 5: Electrochemical performances of the batteries based on **SIP-PC-3**/TEG electrolyte at 25°C (10 wt% TEG). (a) Cycle performance of the Li/LiFePO$_4$ cell at a current rate of 1C; (b) charge–discharge profiles in the potential range from 2.5 to 4.2V, and (c) the reversible capacity at various current rates (C/10 to 1C).

Conclusions

In this work, the electrochemical performance of PEO-SPE has been improved by the incorporation of few carbonyl groups. Innovative functional polycarbonates have been synthesized by organocatalyzed polyaddition of CO2-sourced bis(α-alkylidene carbonate)s (bis-αCCs) with polyethylene oxide diols at room temperature. After analyzing all the polycarbonates designed, the mechanical properties of the best candidate were improved. The SPE with highest ethylene oxide units the most valuable electrochemical properties. After analyzing ionic conductivity(10^{-4} S cm^{-1} at 60 °C) , lithium transference (0.28) number and electrochemical stability (5 V), the battery performance was evaluated at 60 °C with LFP as a cathode. The performance shows a capacity of 83 mAh g^{-1} still after cycling the battery at a C-rate of 1C at 60 °C. These promising results lead in including 10 wt% of tetraglyme in the formulation of SPE with the goal of cycling the battery at rt. Successfully, comparable potential values were achieved at the same experiment conditions but at rt.

Conflicts of interest

In accordance with our policy on Conflicts of interest please ensure that a conflicts of interest statement is included in your manuscript here. Please note that this statement is required for all submitted manuscripts. If no conflicts exist, please state that “There are no conflicts to declare”.

Acknowledgements

C.D. thanks the "Fonds National pour la Recherche Scientifique” (F.R.S.-FNRS) and the Fonds Wetenschappelijk Onderzoek – Vlaanderen (FWO) for financial support in the frame of the EOS project n°O019618F (ID EOS: 30902231). The authors from Liege thank the CESAM Research Unit for financial support. C.D. is F.R.S.-FNRS Research Director.

We are grateful to the financial support of the European Research Council by Starting Grant Innovative Polymers for Energy Storage (iPes) 306250 and the Basque Government through ETORTEK Energigune 2013 and IT 999-16. Leire Meabe thanks Spanish Ministry of Education, Culture and Sport for the predoctoral FPU fellowship received to carry out this work. The authors would like to thank the European Commission for their financial support through the project SUSPOL-EJD 642671 and the Gobierno Vasco/Eusko Jaurlaritza (IT

999-16). The authors thank for technical and human support provided by SGIker of UPV/EHU for the NMR facilities of Gipuzkoa campus.

Notes and references

‡ Footnotes relating to the main text should appear here. These might include comments relevant to but not central to the matter under discussion, limited experimental and spectral data, and crystallographic data.

§

§§

etc.

1 Citations should appear here in the format A. Name, B. Name and C. Name, *Journal Title*, 2000, **35**, 3523; A. Name, B. Name and C. Name, *Journal Title*, 2000, **35**, 3523.

2 …

[1] J. Tollefson, Nature, 2008, 456, 436-440.

[2] M. Armand and J. M. Tarascon, Nature, 2008, 451, 652-657.

[3] Tarascon, J. M.; Armand, M. Issues and Challenges Facing Rechargeable Lithium Batteries. Nature 2001, 414, 359–367.

[4] W. Xu, J. Wang, F. Ding, X. Chen, E. Nasybulin, Y. Zhang and J.-G. Zhang, Energy Environ. Sci., 2014, 7, 513-537.

[5] M. Armand, F. Endres, D. R. MacFarlane, H. Ohno and B. Scrosati, Nat. Mater., 2009, 8, 621.

[6] W. H. Meyer, Adv. Mater., 1998, 10, 439.

[7] D. T. Hallinan and N. P. Balsara, Annu. Rev. Mater. Res., 2013, 43, 503–525.

[8] P. Arora, Z. Zhang, Chemical Reviews 104 (2004) 4419.

[9] J. Y. Song, Y. Y. Wang and C. C. Wan, J. Power Sources, 1999, 77, 183–197.

[10] Xue, Z.; He, D.; Xie, X. Poly(ethylene oxide)-based electrolytes for lithium-ion batteries. *J. Mater. Chem. A.* 2015, *3*, 19218–19253.

[11] L.Y. Yang, D.X. Wei, M. Xu, Y.F. Yao, Q. Chen, Angew. Chem. Int. Ed. 53 (2014) 3631–3635.

[12] E. Quartarone and P. Mustarelli, Chem. Soc. Rev., 2011, 40, 2525–2540.

[13] J. Yuan, D. Mecerreyes and M. Antonietti, Prog. Polym. Sci., 2013, 38, 1009–1036.

[14] J. Kalhoff, G. G. Eshetu, D. Bresser and S. Passerini, ChemSusChem, 2015, 8, 2154–2175.

[15] L. Meabe, T. V. Huynh, N. Lago , H. Sardon, C. Li , L. A. O'Dell , M. Armand, M. Forsyth, D. Mecerreyes. Electrochimica Acta 264 (2018) 367.

[16] Tominaga, Y.; Shimomura, T.; Nakamura, M. Alternating Copolymers of Carbon Dioxide with Glycidyl Ethers for Novel IonConductive Polymer Electrolytes. Polymer 2010, 51, 4295–4298. (b) Nakamura, M.; Tominaga, Y. Utilization of Carbon Dioxide for Polymer Electrolytes II: Synthesis of Alternating Copolymers with Glycidyl Ethers as Novel Ion-Conductive Polymers. Electrochim. Acta 2011, 57, 36–39. (c) Kento Kimura, Mari Yajima, Yoichi Tominaga. A highly-concentrated poly(ethylene carbonate)-based electrolyte for all-solid-state Li battery working at room temperature. Electrochemistry Communications. 66, 2016, 46–48.

[17] Marlena D. Konieczynska, Xinrong Lin, Heng Zhang, and Mark W. Grinstaff. Synthesis of Aliphatic Poly(ether 1,2-glycerol carbonate)s via Copolymerization of CO2 with Glycidyl Ethers Using a Cobalt Salen Catalyst and Study of a Thermally Stable Solid Polymer Electrolyte. ACS Macro Lett. 2015, 4, 533−537

[18] S. Gennen, B. Grignard,T. Tassaing, C. Jérôme,and C. Detrembleur. Angew.Chem. 2017, 129,10530–10534.

[19] Wei Chen, Huicui Yang, Rong Wang, Ru Cheng, Fenghua Meng, Wenxiang Wei, and Zhiyuan Zhon. Macromolecules, 43, 2010, 201.

[20] J. C. Chai, Z. H. Liu, J. Ma, J. Wang, X. C. Liu, H. S. Liu, J. J. Zhang, G. L. Cui, L. Q. Chen, Adv. Sci. 2017, 4, 1600377.

[21] Y. Tominaga, K. Yamazaki, Chem. Commun. 2014, 50, 4448.

[22] W. He, Z. Cui, X. Liu, Y. Cui, J. Chai, X. Zhou, Z. Liu, G. Cui, Electrochim. Acta 225 (2017) 151e159.

[23] Junjie Bao, Gaojian Shi, Can Tao, Chao Wang, Chen Zhub, Liang Cheng, Gang Qian, Chunhua Chen. Journal of Power Sources 389 (2018) 84–92.

[24] Xiaochen Liu, Guoliang Ding, Xinhong Zhou, Shizhen Li, Weisheng He, Jingchao Chai, Chunguang Pang, Zhihong Liu and Guanglei Cui. ***J. Mater. Chem. A***, 2017,

[25] Fadoi Boujioui, Flanco Zhuge, Helen Damerow, Mohammad Wehbi, Bruno Ameduri and Jean-François Gohy. ***J. Mater. Chem. A***, 2018,**6**, 8514-8522.

[26] David G. Mackanic, Wesley Michaels, Min Ah Lee, Dawei Feng, Jeffrey Lopez, Jian Qin, Yi Cui, Zhenan Bao. Adv. Energy. Mater. 8, 2018, 1800703.

[27] Yongfen Tong, Hailong Lyu, Yuzhong Xu, Bishnu Prasad Thapaliya, Peipei Li, Xiao-Guang Sun and Sheng Dai. ***J. Mater. Chem. A***, 2018,**6**, 14847-14855.

[28] Xiaochen Liu, Guoliang Ding, Xinhong Zhou, Shizhen Li, Weisheng He, Jingchao Chai, Chunguang Pang, Zhihong Liu and Guanglei Cui. ***J. Mater. Chem. A***, 2017,

[29] Hyo-Jeong Ha, Eun-Hye Kil, Yo Han Kwon, Je Young Kim, Chang Kee Lee and Sang-Young Lee. ***Energy Environ. Sci.***, 2012,**5**, 6491-6499.

[30] Jijeesh R. Nair, Matteo Destro, Federico Bella, Giovanni B. AppetecchiClaudio Gerbaldi. Journal of Power Sources 306 (2016) 258-267

[31] H. Ben Youcef, O. Garcia-Calvo, N. Lago, D. Shanmukaraj, M. Armand, Electrochim. Acta 2016, 220, 587.

[32] P.-J. Alarco, Y. Abu-Lebdeh, A. Abouimrane, M. Armand, Nat. Mater. 2004, 3, 476.

[33] R. Khurana, J. L. Schaefer, L. A. Archer, G. W. Coates, J. Am. Chem. Soc. 2014, 136, 7395.

[34] L. Long, S. Wang, M. Xiao, Y. Meng, J. Mater. Chem. A 2016, 4, 10038.

[35] C. S. Kim, S. M. Oh, Electrochim. Acta 2001, 46, 1323.

[36] R. C. Agrawal, G. P. Pandey, J. Phys. D.: Appl. Phys. 2008, 41, 223001.

[37] Ziyin Huang, Qiwei Pan, Derrick M. Smith, and Christopher Y. Li. Adv. Mater. Interfaces 2018, 1801445.

[38] David G. Mackanic, Wesley Michaels, Min Ah Lee, Dawei Feng, Jeffrey Lopez, Jian Qin, Yi Cui, Zhenan Bao. Adv. Energy. Mater. 8, 2018, 1800703.

[39] Guopeng Fu and Thein Kyu. Langmuir 2017, 33, 13973−13981.

[40] Hongyun Yue, Jingxian Li, Qiuxian Wang, Chengbin Li,,‖ Jian Zhang, Qianhui Li, Xiangnan Li, Huishuang Zhang, and Shuting Yan. ACS Sustainable Chem. Eng. 2018, 6, 268−274.

[41] Jungdon Suk, Yu Hwa Lee, Do Youb Kim, Dong Wook Kim, Song Yun Cho, Ji Man Kim, Yongku Kang. Journal of Power Sources 334 (2016) 154e161.